

A Search for ELF/VLF Emissions Induced by Earthquakes as Observed in the Ionosphere by the DE 2 Satellite

T. R. HENDERSON,¹ V. S. SONWALKAR, R. A. HELLIWELL, U. S. INAN, AND A. C. FRASER-SMITH

Space, Telecommunications, and Radioscience Laboratory, Stanford University, Stanford, California

Satellite observations of ELF/VLF wave activity by groups from both the Soviet Union and France have indicated the possibility of ELF/VLF radio emissions generated by earthquakes. However, an examination of ELF/VLF wave data from the low-altitude (apogee ~ 1300 km, perigee ~ 300 km, inclination $\sim 90^\circ$) Dynamics Explorer 2 (DE 2) satellite showed no clearly distinguishable ELF/VLF signatures associated with earthquakes. After an initial survey of approximately 5000 DE 2 orbits, ELF and VLF wave data were selected from 63 satellite orbits, called earthquake orbits, in which the ionospheric footprint of the DE 2 crossed the geographic latitude while passing within $\pm 20^\circ$ geographic longitude of the epicenters of imminent or recent earthquakes of magnitude ≥ 5.0 . ELF/VLF noise measured near the epicenters was analyzed for occurrence rates and average spectra, as well as for peak and mean electric field intensities in three spectrometers covering a frequency range of 4 Hz - 512 kHz in 20 channels. The same analysis was then repeated for 61 carefully matched control orbits when there were no imminent or recent earthquakes within $\pm 20^\circ$ geographic longitude or within $\pm 10^\circ$ geographic latitude of the satellite footprint. These control orbits resembled the earthquake orbits with respect to latitude, longitude, local time, and geomagnetic index K_p . Sixty-three percent of the earthquake orbits showed an ELF or VLF emission above $10 \mu\text{V/m}$ in at least one of the 20 channels when the satellite passed near an epicenter. The same analysis performed on control orbit data yielded a 62% chance of observing similar emissions. Moreover, these results did not change when geomagnetic latitudes, instead of geographic latitudes, were considered. Further analyses failed to indicate any significant differences between the ELF/VLF noise measured on earthquake orbits and control orbits with regard to the general nature of the spectra, the frequency of occurrence of emissions, and peak and mean values of the electric field of the emissions.

1. INTRODUCTION

Ionospheric and magnetospheric disturbances attributable to seismic phenomena have been the subject of many investigations in recent years. Ground-based observations of ULF, ELF, and VLF radio emissions associated with seismic activity have been widely documented [Gokhberg *et al.*, 1981; Gokhberg *et al.*, 1982a; Maki and Ogawa, 1983; Tate and Daily, 1989; Fraser-Smith *et al.*, 1990]. Within the last 10 years, several researchers have attributed satellite-based observations of anomalous wide-band ELF/VLF emissions to concurrent earthquake activity near the footprint of the satellite orbital track [Gokhberg *et al.*, 1982b; Larkina *et al.*, 1983; Parrot and Lefeuvre, 1985; Chmyrev *et al.*, 1989; Larkina *et al.*, 1989; Parrot and Mogilevsky, 1989; Serebryakova *et al.*, 1992]. The confirmation of such a result would aid in refining current theories about such issues as earthquake mechanisms, piezoelectric effects in rock, and ELF/VLF wave propagation from ground sources to the ionosphere.

Past satellite observations of ELF/VLF emissions associated with earthquakes can be categorized into two general classes, those using a case study [Gokhberg *et al.*, 1982b; Larkina *et al.*, 1983; Parrot and Mogilevsky, 1989; Larkina *et al.*, 1989; Serebryakova *et al.*, 1992] and those using a statistical approach in which the aggregate ELF/VLF wave data associated with many earthquakes are examined [Parrot and Lefeuvre, 1985; Larkina *et al.*, 1989; Serebryakova *et al.*, 1992]. Investigations of particular cases, in which anomalous rises in the ELF/VLF spectrum on a particular

orbit or a set of successive orbits of the Intercosmos 19 satellite were associated with a nearby large earthquake ($5.0 \leq m_b \leq 6.1$), have been detailed by Larkina *et al.* [1983]. More recent studies by Parrot and Mogilevsky [1989], using the Aureol 3 satellite, and by Larkina *et al.* [1989], again using the Intercosmos 19 satellite, used the same case study approach. All of these studies indicated that as the polar orbiting satellites crossed the geographic (or in some cases geomagnetic) latitude of a strong earthquake, a short (approximately 1-3 min) but sharp rise and fall of the background noise intensity level occurred in many electric field and magnetic field ELF/VLF channels. As Larkina *et al.* [1989] illustrated, the noise was distributed along "longitudinal noise belts" over $\pm 60^\circ$ in longitude and $\pm 2^\circ$ in latitude from the earthquake epicenter and could be observed for several hours before or after the earthquake occurred. Similarly, Parrot and Mogilevsky [1989] measured a rise of ELF/VLF noise near the latitude of an imminent earthquake but at a closer range in both time and space to the earthquake time of occurrence and the epicenter location to which it was attributed. Although control orbits or quantitative measures of normal background emissions have not been cited, the authors claim that such emissions in the low magnetic latitudes are uncommon.

Statistical analyses of a large number of earthquakes were performed in two instances. Larkina *et al.* [1989] assembled a set of ~ 150 orbits associated with 39 earthquakes (several orbits per earthquake, with successive orbits separated in time by the ~ 100 -min orbital period of the Intercosmos 19 satellite) to look for the reliability and repeatability of this phenomenon. The measurements near an earthquake epicenter were assigned a weight according to the strength of the emission and its latitudinal displacement with respect to the epicenter. The calculated reliability of the precursor and postcursor emissions, based on experimental observation, ranged from 0.8 to 0.9. These reliability figures

¹Now at COMSAT Laboratories, Clarksburg, Maryland.

do not include control orbits but instead attempt to determine the likelihood that such observed emissions did not randomly group near the epicenters, based on Gaussian probability distributions. However, the unconditional probability of an electric field emission near an epicenter as a function of the emission's frequency was somewhat lower, ranging from 0.49 to 0.69. Using the geostationary satellite GEOS 2, *Parrot and Lefevre* [1985] also performed a large statistical study on the probability of occurrence of a VLF emission rise when earthquakes occurred near the magnetic footprints of the spacecraft. A total of 296 earthquakes with magnitude >4.7 at longitudes $\pm 40^\circ$ with respect to the north and south footprints of GEOS-2 were examined for short term (15 min before or after an earthquake) increases in average wave activity as compared to long term (90 min; 45 min before and 45 min after an earthquake) average wave activity. A positive correlation was attributed to 44.3% of all cases, compared with a correlation of 41.4% in a control study of random data (353 randomly selected periods). However, when using only the 152 earthquakes within $\pm 20^\circ$ geographical longitude of the GEOS 2 ionospheric footprints, a positive correlation is attributed to 51.3% earthquake events. The authors concluded that there appears to be an association between VLF emissions observed on satellites and seismic activity.

More recent work by *Serebryakova et al.* [1992] examined a number of case studies connected with one active earthquake region. Twenty-four orbits were examined that passed within 12° in longitude of the epicentral region in Armenia during the months following the primary shock of December 7, 1988. Magnetic field emissions were observed as the satellite Cosmos 1809 crossed the same geomagnetic latitude as the epicentral region, but only at longitudes within 6° to 8° of the region. The authors concluded that the epicentral region was permanently radiating at this time due to the many aftershocks in this region. These particular orbits were combined with the data from orbits of the Aureol 3 spacecraft near other epicenters to define a power spectrum, which was then compared with the average power spectrum recorded by Aureol 3 at low magnetic latitudes.

Satellite-based detection of ELF/VLF waves associated with seismic activity is difficult for two reasons: (1) the chances of a polar orbiting satellite performing ELF/VLF measurements near the epicenter of a large imminent or recent earthquake are small, and (2) the spectral signature of the earthquake related emission has to be clearly distinguishable from a large variety of ELF/VLF emissions due to sources other than seismic activity (e.g., thunderstorm generated whistlers, hiss, or chorus). The recognition of these difficulties implies that a large amount of data, based on both satellite ELF/VLF measurements and earthquake epicenter listings, has to be examined to select ELF/VLF data that is recorded near an imminent or recent earthquake, and more importantly, a large enough data set of control measurements must be carefully selected to provide information on the ELF/VLF noise background originating in nonseismic sources, against which any possible emissions associated with earthquakes can be compared.

This study, using the ELF/VLF data from the DE 2 satellite, attempts to overcome the main drawback of the previous work; namely, the lack of sufficient control data to provide information about normal low-latitude ELF/VLF background emissions. An analysis of ELF/VLF wave data is presented using comparable sets of earthquake and control orbits as detailed in the next section.

2. EXPERIMENTAL METHOD

2.1. The Dynamics Explorer 2 Satellite

The Dynamics Explorer Program was designed to investigate coupling and interaction between the hot plasmas of the magne-

tosphere and the cooler plasmas of the plasmasphere, ionosphere, and upper atmosphere [*Hoffman et al.*, 1981]. Both the high-altitude DE 1 and the low-altitude polar DE 2 satellites were launched and began measurements in 1981, with DE 2 reentering in 1983 and DE 1 discontinuing operations in 1991. An initial attempt to use the wideband VLF data from the DE 1 satellite revealed that, because of its highly elliptic orbit, low-altitude measurements were too infrequent. On the other hand, the DE 2 satellite data consist entirely of low-altitude measurements, but with spectrometers consisting of narrow-band discrete channels, thus lacking the wave spectra detail available with a wideband receiver.

Because matching suitable earthquakes with close-passing satellite orbits requires large quantities of data, the DE 2 satellite proved to be more useful than a higher-altitude satellite such as the DE 1 (apogee $\sim 25,000$ km). The DE 2 satellite was in a polar orbit with an initial apogee and perigee of 1300 km and 305 km, respectively, and with a period of 101 min [*Hoffman et al.*, 1981]. This type of satellite is well suited for this study because it orbited many times daily, crossing low geomagnetic latitudes. The DE 2 Z axis was usually along the orbit normal, the spacecraft Y axis was always held parallel or antiparallel to nadir, and the spacecraft X axis was determined by the right-hand rule and in the approximate direction of the velocity vector. Orbital parameters of the DE 2 spacecraft were, in general, similar to those of the Intercosmos 19, Cosmos 1809, and Aureol 3 satellites used in previous earthquake research (for a full description of the DE 2 experiment, see *Space Science Instrumentation* (volume 5, 1981)).

2.2. The Vector Electric Field Instrument

The vector electric field instrument (VEFI) was designed to provide large dynamic range, high temporal/spatial resolution, triaxial electric field measurements. Six-11-m long cylindrical antennas were planned to be deployed along three axes to form an array, with the Z antenna along the spacecraft Z axis and the X and Y antennas at 45° to the spacecraft's X and Y axes, respectively. In orbit, however, one Z axis antenna failed to deploy, and measurements were limited to the X and Y electric field axes. AC electric field measurements were performed in a $1 \mu\text{V/m}$ to 10 mV/m range. The AC portion of the VEFI was comprised of a filter bank of 20 channels, separated into two groups of eight channels covering the frequency range from 4 Hz to 1 kHz and one group of 4 channels covering from 1 kHz to 512 kHz. Quantitative spectral plots for all of the channels on a given orbit were obtained using three comb filter spectrometers. For the 16 channels between 4 Hz and 1 kHz (spectrometers A and B), both peak and rms values were recorded either once or twice per second, while for the four VLF channels from 1 kHz to 512 kHz (spectrometer C), only rms values were recorded either once or twice per second. In the spectrometer's high gain setting, sensitivity was approximately $1 \mu\text{V/m}$ (independent of filter bandwidth), while in the low-gain setting, sensitivity was approximately $10 \mu\text{V/m}$ (see Table 1) [*Maynard et al.*, 1981].

The general mode of operation of the VEFI was to assign spectrometers A and C to the axis nearest to perpendicular to the magnetic field. Spectrometer B was generally assigned to the axis nearest to parallel to the magnetic field. On occasion, all three spectrometers were assigned to the same axis. The DE 2 VEFI instrumentation was comparable to the satellite spectrometers used in previous earthquake research [*Maynard et al.*, 1981; *Larkina et al.*, 1983; *Parrot and Mogilevsky*, 1989]; it had comparable sensitivity on the electric field component (AC magnetic fields were not measured) and a wider frequency bandwidth. Consequently, it was assumed that signals reported by previous authors

TABLE 1. Normalized Spectrometer Sensitivity, Based on a Lower Threshold of $10 \mu\text{V/m}$, for the 20 VEFI Channels

Channel	Bandwidth	Normalized Lower Threshold, $\mu\text{V/m Hz}$
<i>Spectrometer C</i>		
128 - 512 kHz	384 kHz	0.016
16 - 64 kHz	48 kHz	0.045
4 - 16 kHz	12 kHz	0.09
1 - 4 kHz	3 kHz	0.18
<i>Spectrometer A</i>		
512 - 1024 Hz	512 Hz	0.43
256 - 512 Hz	256 Hz	0.63
128 - 256 Hz	128 Hz	0.88
64 - 128 Hz	64 Hz	1.3
32 - 64 Hz	32 Hz	1.8
16 - 32 Hz	16 Hz	2.5
8 - 16 Hz	8 Hz	3.6
4 - 8 Hz	4 Hz	5.0
<i>Spectrometer B</i>		
512 - 1024 Hz	512 Hz	0.43
361 - 512 Hz	151 Hz	0.82
256 - 361 Hz	105 Hz	0.98
181 - 256 Hz	75 Hz	1.15
64 - 128 Hz	64 Hz	1.25
45 - 64 Hz	19 Hz	2.3
16 - 32 Hz	16 Hz	2.5
4 - 8 Hz	4 Hz	5.0

would be observed on the DE 2 satellite, provided that the satellite footprint passed sufficiently close to the epicenters of comparable earthquakes within a sufficiently close time frame with respect to the shock, as reported in past works [Larkina et al., 1989; Parrot and Mogilevsky, 1989].

2.3. Data Selection for Earthquake-Coincident Orbits

Orbits for this study were selected based on criteria similar to those used in the previous research discussed above. The following criteria were used to select DE 2 orbits for this study:

1. Satellite passed over the geographic latitude of an earthquake epicenter and within $\pm 20^\circ$ of the epicenter's geographic longitude. Previously reported emissions associated with earthquake activity were observed over a wide range of longitude centered within a few degrees of latitude of the earthquake epicenter. For example, the emissions were seen over $\pm 60^\circ$ in longitude from an epicenter [Larkina et al., 1983] but were stronger at close range [Larkina et al., 1989; Parrot and Mogilevsky, 1989].
2. Satellite passed near an epicenter no more than 12 hours before or 6 hours after an earthquake. Larkina et al. [1983 and 1989] associated individual emissions with a particular earthquake many hours before and after the earthquake occurred.
3. Earthquake body wave magnitude $m_b \geq 5.0$. In the gathering of large numbers of satellite orbits for statistical analyses, similar cutoff criteria for the selection of sufficiently strong earthquakes were used by Parrot and Lefevre [1985] and Larkina et al. [1989].
4. Invariant latitude of the earthquake $\leq 45^\circ$. Auroral hiss and other magnetospheric emissions dominate the VLF spectrum at higher geomagnetic latitudes [Larkina et al., 1989].
5. K_p 3-hour index $\leq 3+$. To avoid the variability in the general ionospheric noise background resulting from geomagnetic disturbances, only geomagnetically "quiet" or "normal" periods are being considered, as in Larkina et al. [1983]. The 3-hour

geomagnetic index has been tabulated by *Geomagnetic and Solar Data* [1981-1983] published in the *Journal of Geophysical Research*.

6. Receiver gain setting on "high" for the VLF channels. Sometimes the VEFI was set on "low" gain to avoid saturating the receiver in the auroral regions. The "high" gain setting provided maximum sensitivity and provided a common context for noise event analysis.

In selecting orbits, epicenter listings from *Preliminary Determination of Epicenters, National Earthquake Information Service* [1981-1983] were used to list all magnitude $m_b \geq 5.0$ earthquakes for a given day. Then, DE 2 summary plot data were scanned to see if the satellite was sufficiently close in time and space to an epicenter. If these criteria were met, and if the spectrometers were operating at the time, the orbit was checked against the remaining criteria for inclusion in the study.

Since the summary plots were intended solely for survey use, complete data were requested from Goddard Space Flight Center for the more detailed analysis that follows. Out of a survey of over 5000 orbits, 58 orbits satisfied the selection criteria. Of these 58 orbits, 63 distinct segments of these orbits could be matched to specific earthquakes, since on four orbits the satellite passed sufficiently close to different earthquakes at more than one latitude. A segment of an earthquake or control orbit is defined as a 4 min portion of the orbit centered on the latitude (geographic or geomagnetic, depending on which is being considered) of an earthquake, during which time the satellite geographic footprint crossed approximately 16° of latitude. The 63 earthquake orbit segments used in this study are hereafter referred to as earthquake orbits.

2.4. Data Selection for Control Orbits

Contrary to previous claims that ELF/VLF emissions at low magnetic latitudes, where all of the earthquake epicenters used in this study were located, are not frequent [Larkina et al., 1989; Parrot and Mogilevsky, 1989], such emissions were observed on DE 2 rather frequently. Therefore it was crucial to analyze control data for orbits that were similar to the candidates for earthquake emissions. All control orbits met criteria 4-6 of section 2.3 for earthquake orbits. In addition, only orbits in similar temporal/spatial locations to the earthquake orbits were used. To be counted as a control orbit, the satellite orbital track had to be within $\pm 10^\circ$ in longitude and within ± 2 hours local time of an earthquake orbit that was previously selected by the above methodology. For example, if a potential control orbit crossed 100° longitude at 1000 local time, it was included only if there was an earthquake orbit used in the study that occurred within both the local time range 0800 to 1200 and the longitude range 90° to 110° . These criteria insured that only control orbits close in local time and geographic location to the earthquake orbits were selected.

Most importantly, control orbits could not have an earthquake of any magnitude within $-12/+6$ hours, $\pm 10^\circ$ latitude, and $\pm 20^\circ$ longitude of the location to which the control orbit is being matched to an earthquake. This exclusion of all earthquakes was subject to the limitations of the U.S. Geological Survey Preliminary Determination of Epicenters, which generally listed all earthquakes greater in magnitude than $m_b = 4.5$ and which also listed smaller magnitude earthquakes where possible (M. J. S. Johnston, personal communications, 1992). In summary, control orbits were selected to match the earthquake orbits as closely as possible, except that for control orbits there were no significant earthquakes near the relevant latitudes.

A total of 45 control orbits were selected, from which a total of 61 distinct orbital segments could be matched to one or

more earthquakes. The 61 control orbit segments are hereafter referred to as control orbits. Because of limited operation of the DE 2 spacecraft due to power constraints and of variations in the magnetic activity, it was difficult to obtain a control orbit for each specific earthquake orbit segment. Nevertheless, 71% of the earthquake orbits can be paired with at least one control orbit. Some of the control orbits matched with more than one earthquake. In general, it is believed that, taken as an aggregate, the control orbit data set provides average ELF/VLF wave activity under geophysical conditions similar to those for the earthquake orbits data set.

2.5. Electric Field Irregularities at Low Magnetic Latitudes

In general, emissions observed in the lower magnetic latitudes were orders of magnitude weaker than those observed in the higher magnetic latitudes. For this reason, the selection of data for this study was confined to periods in which the satellite was in the lower magnetic latitudes. However, even at the lower magnetic latitudes, there exist electric field irregularities that could possibly be misinterpreted as emissions generated by earthquakes. These irregularities have been documented by *Holtet et al.*, [1977] and *Kelley and Mozer*, [1972] and are most commonly found in the 2000-0600 local time sector and near the magnetic equator [*Holtet et al.* 1977]. For this study, since it was not desirable to eliminate the 27 earthquake orbits and 22 control orbits that occurred during this time sector, an attempt was made to screen out such

irregularities from the data set based on their identified signatures. Also, in section 3.2 below, a subset of the data was considered that did not include orbits from the 2100-0500 local time sector.

3. OBSERVATIONS AND INTERPRETATIONS

3.1. Case Studies

Since case studies have formed the bulk of previous works, the data for several individual orbits will now be presented. Figures 1-5 illustrate portions of the VEFI AC spectrometer records for selected DE 2 orbits. Further details of the satellite ephemeris data and earthquake information are given in Table 2. Data from the DE 2 spectrometers are given for all 20 channels; the channels are shown as stacked on top of one another, and the field strengths are given along the vertical axis. Horizontally, each data sample represents an 8 min (left to right) segment of the orbit, during which time the satellite traversed a range of approximately 30° of geographic latitude while maintaining approximately the same geographic longitude. These segments are approximately centered on the geographic and geomagnetic latitude of the earthquake under consideration, and for control orbits, these segments are centered on the geographic and geomagnetic latitude of the earthquake orbit to which the control orbit was matched.

3.1.1. Case study 1: Possible associated emission . Figure 1 shows an 8-min segment of data from orbit 4513, in which the satellite passed within 2.5° longitude of the epicenter of an earth-

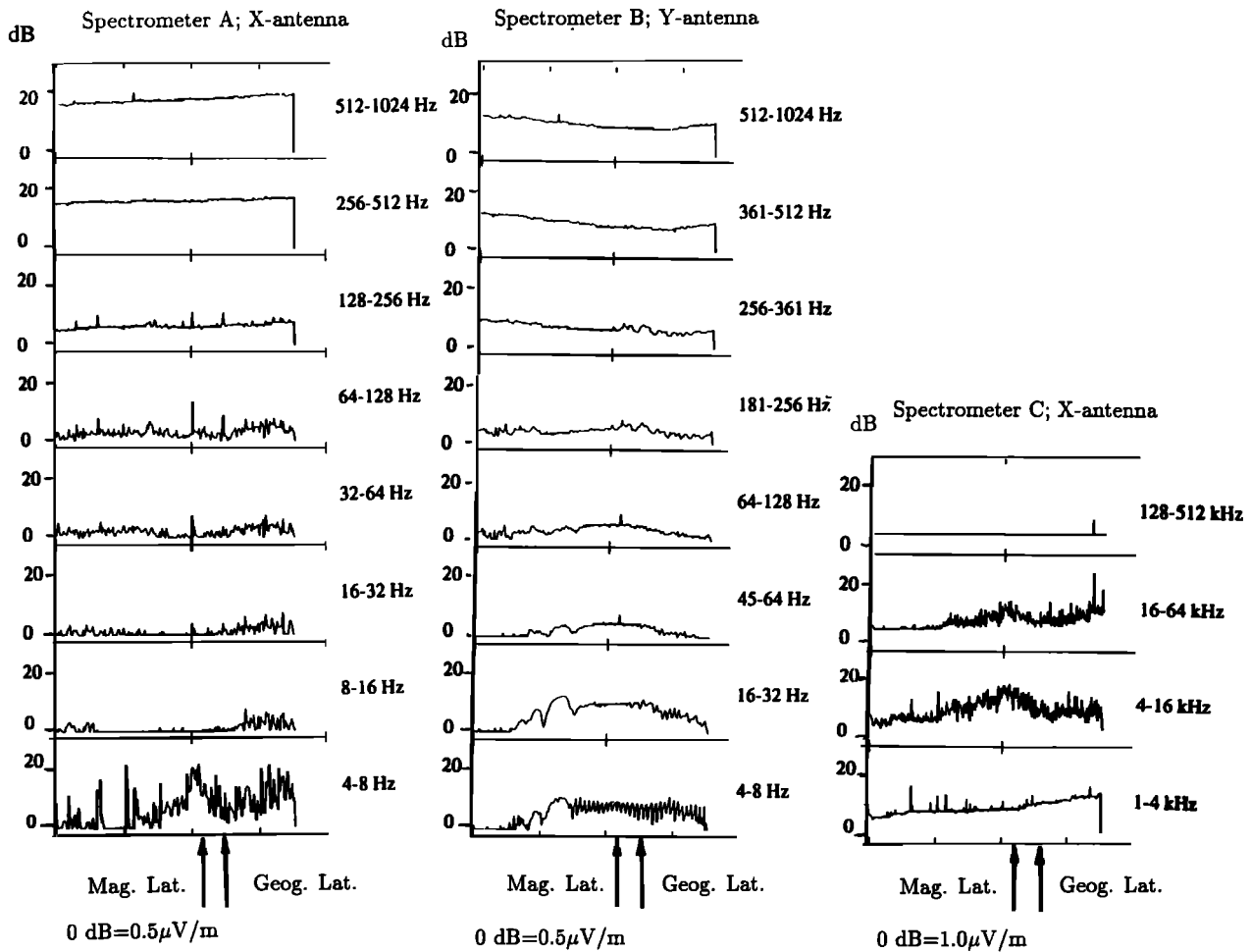


Fig. 1. VEFI data for a 8-min segment of orbit 4513 (see Table 2).

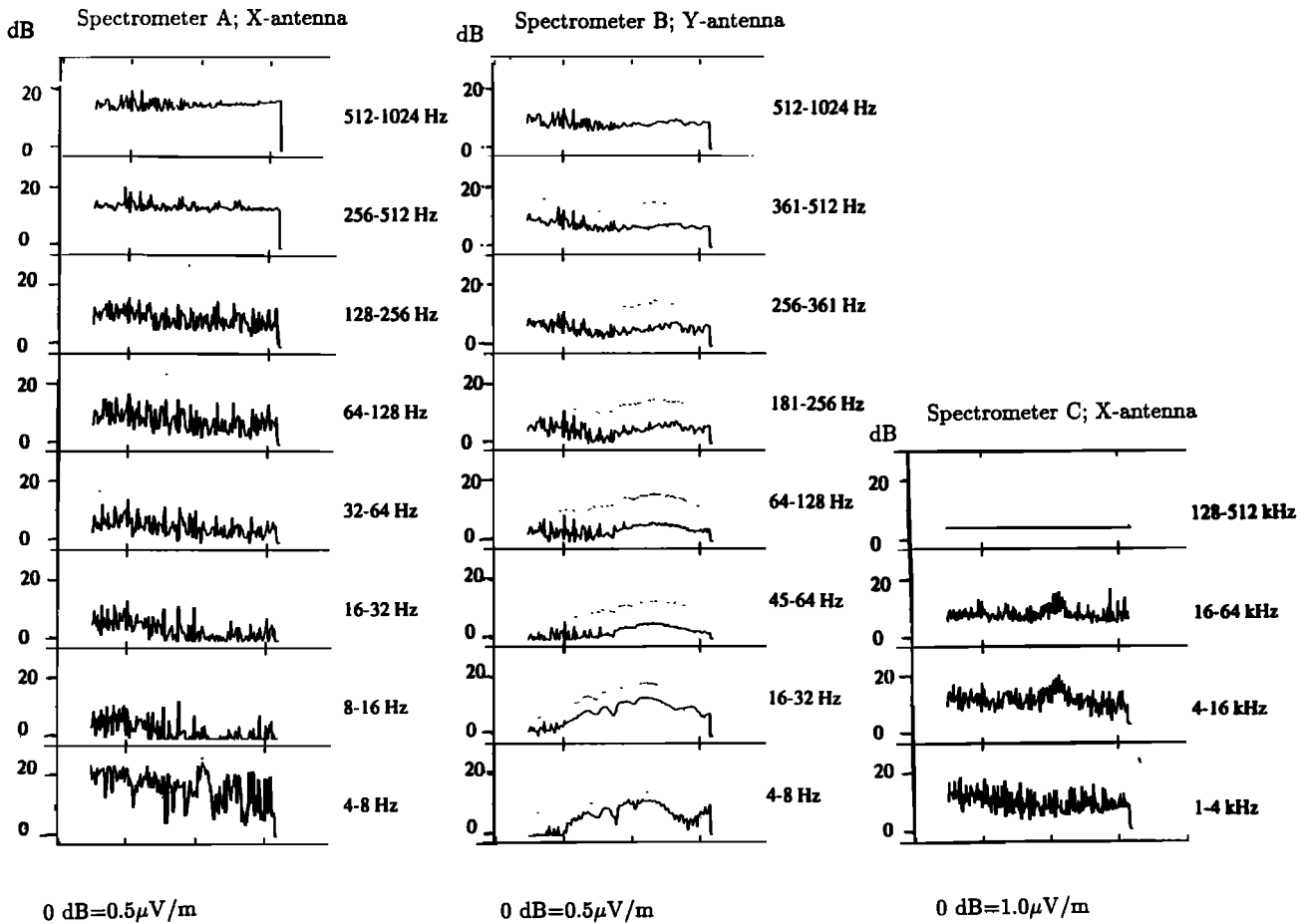


Fig. 2. VEFI data for a 8-min segment of orbit 4528 (see Table 2).

quake 56 min after it occurred. Arrows indicate when the satellite footprint crossed the geographic and magnetic latitude of the earthquake. The magnitude 5.4 earthquake was located in Argentina. Ephemeris data for the satellite, along with earthquake data, are shown in Table 2.

As can be seen from the figure, there is significant wave activity on many channels. At the middle of the plot, which corresponds to a point near the magnetic latitude of the earthquake, a rise and fall in the background noise intensity can be seen in several channels below 32 Hz and in the VLF channels between 4 and 64 kHz. The emissions measured on the 4-8 Hz channel of spectrometer B appear to be spin modulated as well. The presence of emissions at this latitude suggests the possibility that the earthquake which occurred 56 min prior to this orbital pass may have been responsible. Of the 11 earthquake orbits in which the earthquake occurred below land, this is the most likely candidate for an associated emission.

In order to assess the possible normal background emissions on the earthquake orbit segment of Figure 1, data from two control orbits at similar local times and positions are presented in Figures 2 and 3. Ephemeris data for these orbits are presented in Table 2. The first control orbit, shown in Figure 2, occurred almost 24 hours after the orbit shown in Figure 1. Although there had been no earthquake activity in this area on this day, strong emissions are again seen in many of the same channels. The presence of such emissions suggests that electromagnetic effects of the earthquake activity may have still been ongoing or that these emissions

are actually normal background emissions originating from other sources.

The second control orbit, shown in Figure 3, occurred 19 days after the earthquake orbit of Figure 1. The emissions appear weaker in spectrometers A and B, but this is a result of the spectrometer being at a lower gain setting. This difference is shown in the different base of the vertical scale in this figure. Emissions of similar magnitude to Figure 1 were again observed on these channels as they rose above the threshold of $10 \mu\text{V/m}$. The strength of the emissions observed in spectrometer C (same vertical scale as in Figures 1 and 2) is similar to that of Figures 1 and 2. On the basis of the observation during the control orbits of similar emissions in the same channels as those of Figure 1, it becomes difficult to attribute the emissions observed in Figure 1 to the nearby earthquake.

3.1.2. *Case study 2: Absence of an associated emission*. Figure 1, and the corresponding Figures 2 and 3, illustrate orbits in which strong emissions above the receiver threshold were measured. Figure 4 illustrates a case in which such emissions were not measured. On this segment, from orbit 5691, the satellite passed within 17° of longitude of an earthquake epicenter 59 min before it occurred. This earthquake, located in Venezuela, also had a magnitude of 5.4. Again, ephemeris data for the satellite, along with additional earthquake data are shown in Table 2.

In this case there are hardly any emissions measured above the threshold of $10 \mu\text{V/m}$. If emissions associated with earthquake as documented by previous investigators occur with a high

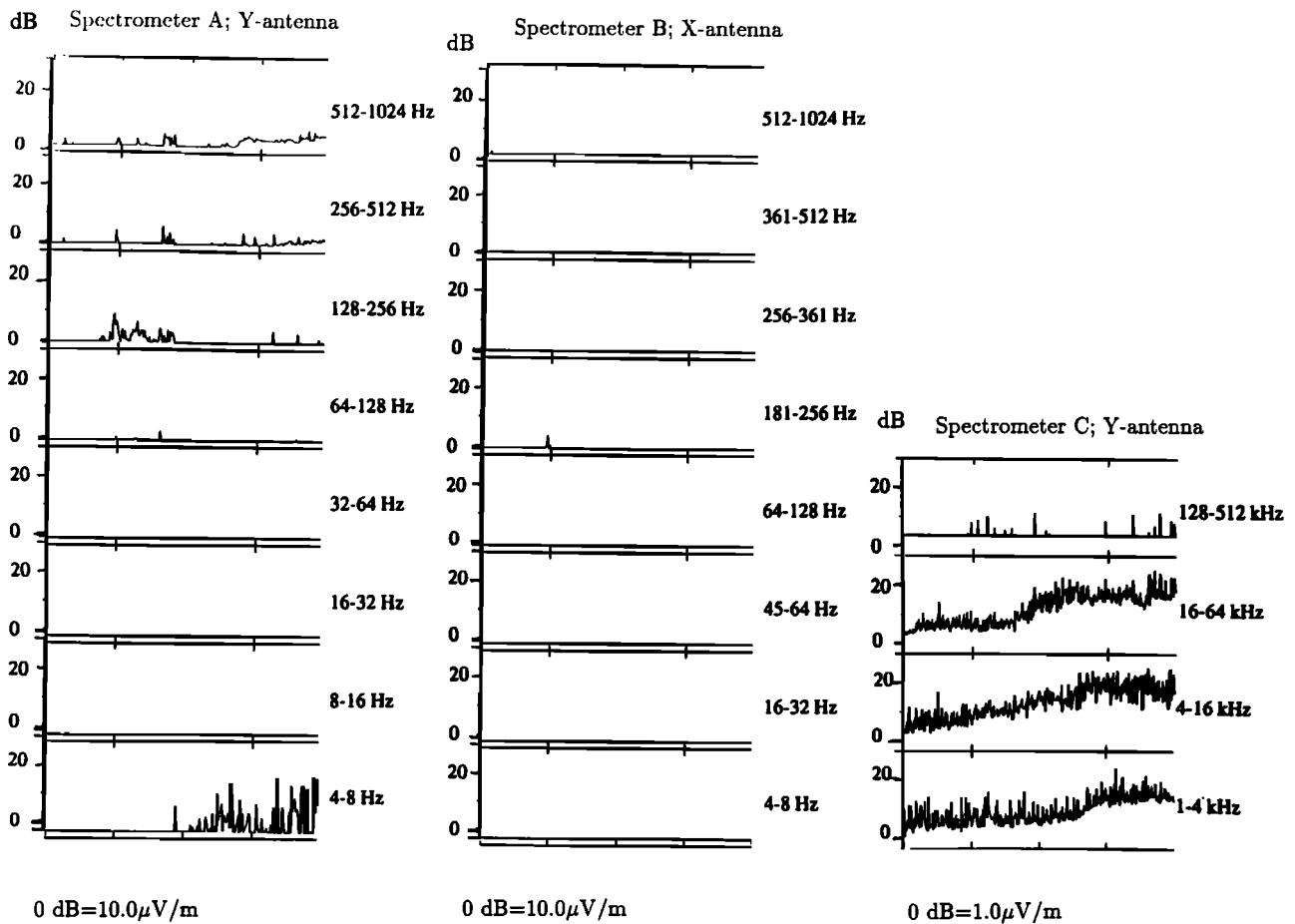


Fig. 3. VEFI data for a 8-min segment of orbit 4801 (see Table 2).

degree of reliability, they should be expected on this orbit. In fact, however, many of the earthquake orbits in this study lacked measurable emissions just as does this orbit. Further, a matched control orbit, illustrated in Figure 5, from 8 days later also lacks strong emissions.

In summary, based on our qualitative analysis none of the earthquake orbits, especially when compared to control orbits, exhibited unusual emissions that could be confidently attributed to a nearby earthquake.

3.2. Statistical Analyses

Case studies provide useful examples, but statistical analyses of the emissions observed near earthquake epicenters as compared to those observed on control orbits are more important, since such seismically related emissions, should they exist, must be distinguished from the average ELF/VLF background emissions. In examining many events, the same criteria must be applied when comparing one event to another. Therefore in interpreting the complete spectra for all 63 earthquake orbits and 61 control orbits, the maximum rms emission magnitude was graphically measured for a 15° latitude (4 min) segment of the orbit. The particular 15° portion was selected so that the 15° latitude range was centered on the epicenter's geographic latitude. Control orbits that were matched to particular earthquake orbits were analyzed along the same 15° latitude segments.

Receiver lower threshold was defined as $10 \mu\text{V/m}$ amplitude, since this was the greatest sensitivity achievable in spectrometers

A and B for most of the orbits. Spectrometer c's four VLF channels were sensitive to $1 \mu\text{V/m}$, but in order to provide a uniform threshold for this statistical comparison, the lower threshold was considered to be $10 \mu\text{V/m}$ even on these channels. This threshold still provided a bandwidth-normalized sensitivity of at least $0.2 \mu\text{V/m (Hz)}^{-1/2}$ in these four VLF channels.

3.2.1. *Aggregate statistics for all orbits*. Figure 6 illustrates the temporal and spatial distribution of the 63 earthquake orbits with respect to their corresponding epicenters. It also presents information concerning orbits that measured emissions on at least one channel. If the particular segment of spectra near the earthquake epicenter showed an emission in excess of $10 \mu\text{V/m}$ rms on at least one channel, the orbit was credited with having an emission. In Table 3, the fraction of orbits showing emissions in the vicinity of the epicenter is denoted for each particular category. For example, 3 of the 63 earthquake orbits passed within 5° longitude of an epicenter from between 8 to 12 hours before the earthquake occurred, and two of these three orbits showed an emission above $10 \mu\text{V/m}$ on at least one channel. The fractions at the end of each row or column are sums for that particular row or column.

Although the spread is fairly uniform, there is a slight tendency for a higher proportion of orbits to exhibit emissions when the satellite is closer in time to the earthquake time of occurrence (6/7 for less than one hour before) or space (29/40 for within 10° geographic longitude) to the earthquake epicenter. However, in overall terms, control orbits were as likely to exceed lower spectrometer thresholds as were earthquake orbits. Forty of 63

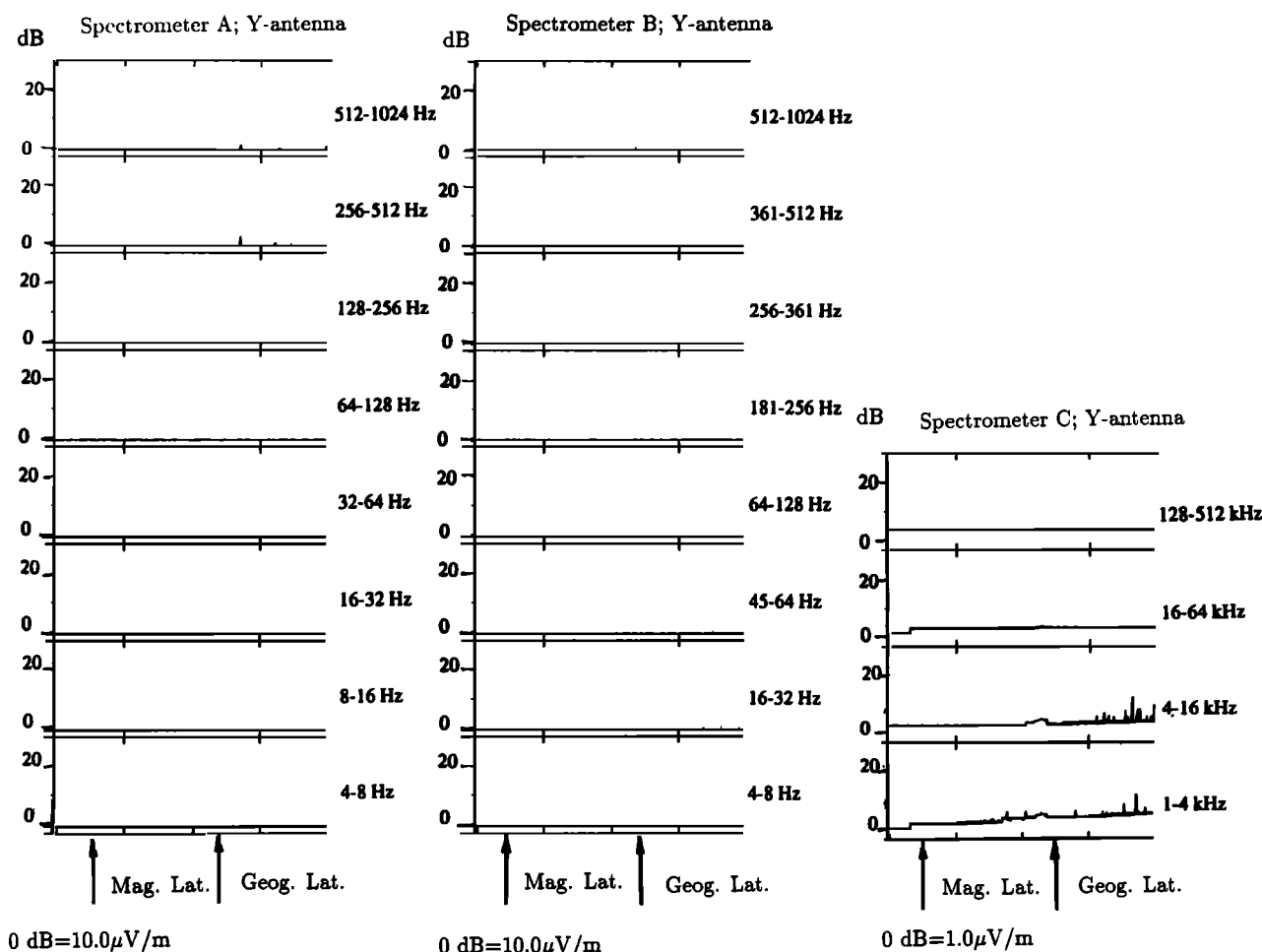


Fig. 4. VEFI data for a 8min segment of orbit 5691 (see Table 2).

earthquake orbits (63%) showed some kind of emission in at least one channel; when the control orbit segments are similarly analyzed, 38 of 61 (62%) showed an emission in at least one channel. These results illustrate two features of the data, based on this particular measure: (1) observations closer in time or longitude to the earthquake epicenters appear, at first glance, to be more likely to exhibit some kind of emission than observations further separated from the earthquake epicenters, and (2) taken as a group, satellite orbits included in this study do not exhibit statistics different from those of control orbits.

Figure 7 illustrates the fraction of earthquake orbits and control orbits exceeding the $10\text{-}\mu\text{V/m}$ threshold for all 20 channels as a function of the channel. A few general trends can be seen from this figure. First, for both earthquake and control orbits, emissions above the threshold were most common in the range from 0.5 kHz to 64 kHz, while relatively fewer orbits exceeded this threshold for channels at lower or higher frequencies. Second, control orbits exceeded the threshold, on average, slightly more than did the earthquake orbits. Overall, however, there is no significant difference between the group of earthquake orbits and the control orbits; the small differences are probably due to the sample size of the data set.

A measure of the strengths of these emissions as a function of channel is illustrated by Figures 8 and 9. As discussed above, only a fraction of the orbits exceeded the lower spectrometer threshold. If an orbit did exceed the threshold for a particular channel, the

maximum field strength was measured. Figure 8 is a plot of the maximum value reached on a particular channel considering all 63 earthquake orbits and all 61 control orbits. Figure 9 is a plot of the mean value of those emissions that exceeded the threshold. For example, if 20 of the 63 orbits exceeded the threshold for a particular channel, the largest of the 20 values is plotted in Figure 8 and the mean of the 20 values is plotted in Figure 9. These figures represent, in a sense, average spectra for the observed emissions for earthquake and control orbits. They illustrate, particularly in the plot of mean value versus, channel, that the strengths of emissions measured on earthquake orbits do not differ significantly from those measured on control orbits. More distinct differences between earthquake orbits and control orbits illustrated in the graph's ELF range are probably due to the very small sample size from which data for these particular channels are drawn (refer to Figure 7); there were very few emissions that exceeded the threshold in these channels).

3.2.2. *Aggregate statistics using geomagnetic coordinates*. Some previous authors [Serebryakova et al., 1992] have observed anomalous emissions occurring at the same geomagnetic, instead of geographic, latitude as that of an earthquake. For this reason, the same analysis as above has been repeated but by using the geomagnetic latitude of the epicenter as a criterion instead of the geographic latitude. This new criterion limited the data set somewhat, since the magnetic footprint of the DE 2 satellite often did not cross very low invariant latitudes, where some of

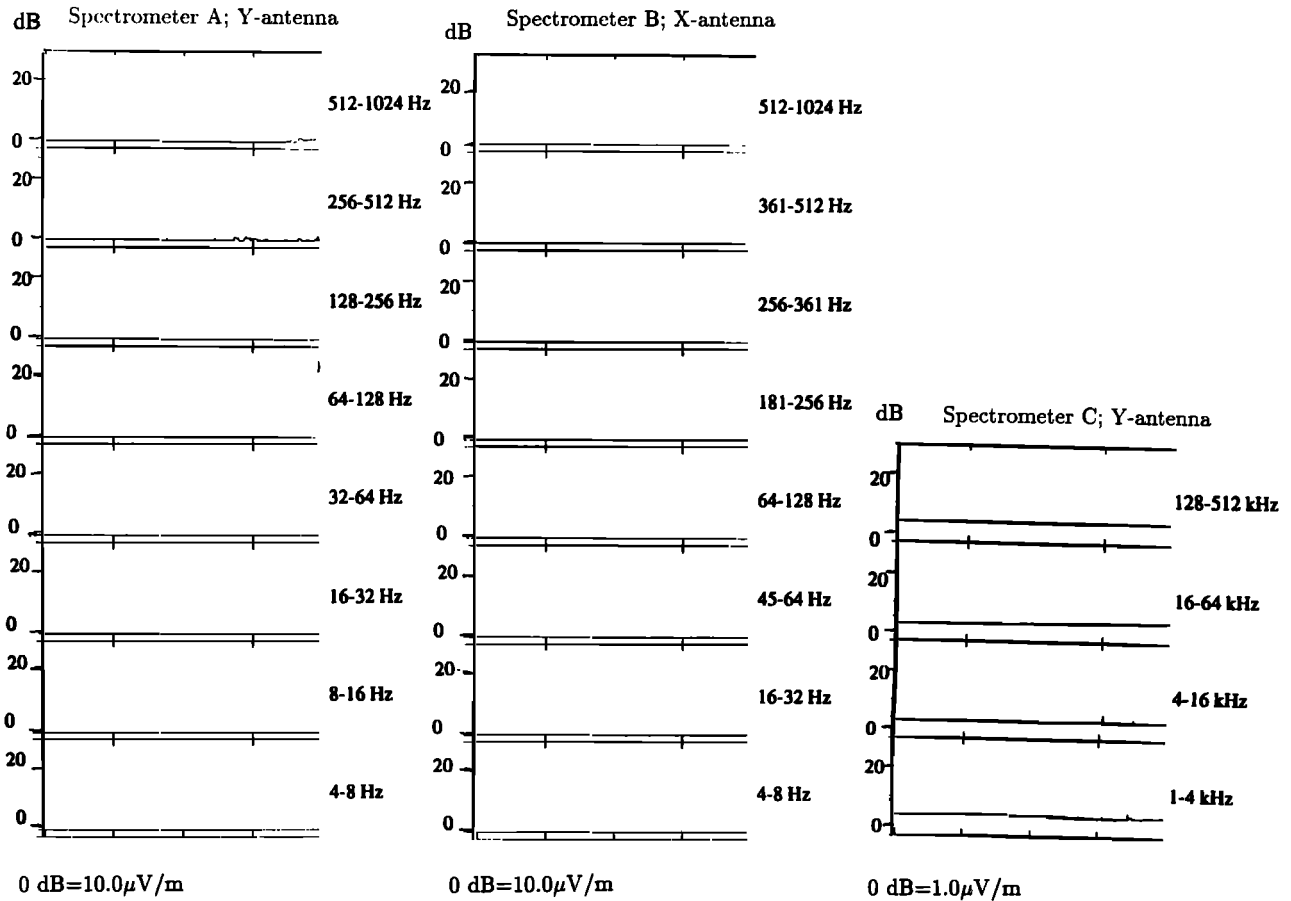


Fig. 5. VEFI data for a 8-min segment of orbit 5813 (see Table 2).

TABLE 2. Satellite Ephemeris and Earthquake Data for Figures 1-5

	Figure 1	Figure 2	Figure 3	Figure 4	Figure 5
<i>Satellite Data</i>					
Date	June 1, 1982	June 2, 1982	June 20, 1982	Aug. 17, 1982	Aug. 25, 1982
Time range, UT	1028-1036	1010-1018	912-920	1720-1728	1634-1642
Orbit number	4513	4528	4801	5691	5813
Geographic latitude	23.8° S-	23.3° S-	23.0° S-	9.4° S-	4.5° S-
latitude range	55.6° S	55.1° S	52.7° S	20.5° N	24.9° N
Geographic longitude	66° W-	63° W-	65° W-	65° W-	63° W-
longitude range	68° W	65° W	67° W	67° W	65° W
Magnetic latitude	21° S-	22.1° S-	23.7° S-	20° N-	24° N-
latitude range	43.4° S	42.3° S	42.4° S	38° N	41.2° N
Local time	1742	1742	1630	1256	1224
Altitude, km	318-413	325-424	538-653	547-654	632-658
Kp 3-hour index	2	2	3	1	3
<i>Earthquake Data</i>					
Date	June 1, 1982			Aug. 17, 1982	
Time, UT	0937:25			1824:05	
Geographic latitude	42.87° S			9.54° N	
Geographic longitude	70.34° W			84.16° W	
Magnetic latitude	31.9° S			20.2° N	
Magnitude, M_b	5.4			5.4	
Location	Argentina (land)			Venezuela (land)	
Depth, km	33			33	
Orbit separation in longitude	2.5°			17	
Orbit separation in time, hours	0:56 after earthquake			0:59 before earthquake	

		Separation in longitude (degrees)				Row sums:
		0-5	5-10	10-15	15-20	
Before earthquake	8-12	2/3	6/6	1/3	0/2	9/14
	6-8	0/1	1/1	0/1	1/1	2/4
	4-6	2/3	0/1			2/4
	2-4	2/2	1/3	2/2	1/1	6/8
	1-2	1/1		1/1	0/1	2/3
	0-1	2/3	3/3		1/1	6/7
	Column sums:		13/19	16/21	5/12	6/11
After earthquake	0-1	1/1	1/2	0/3	0/1	2/7
	1-2	1/1	0/1	1/2	1/1	3/5
	2-4	1/2	3/3		2/3	6/8
	4-6	1/2	1/1			2/3

FIG. 6. Distribution of the 63 earthquake orbits with respect to their associated earthquakes when DE 2 crossed the geographic latitude of the earthquake. The fractions in each box, row, or column represent the fraction of orbits within that particular category which measured an emission exceeding 10 μ V/m in at least one channel. Sixty-three percent of earthquake orbits measured at least one such emission, compared with 62% of control orbits.

the earthquakes were located. Nevertheless, 41 earthquake orbits and 28 control orbits could be selected under these criteria. Figure 10 illustrates the fraction of orbits during which there was an observed emission near the magnetic latitude of an earthquake, compared with appropriately matched control observations. As can be seen in comparison with Figure 7, emissions were again observed near epicenters slightly less often than when geographic latitude was the criterion used, particularly in the channels between 1 and 16 kHz. Furthermore, qualitative examination of

these 41 orbits yielded no unusual emissions occurring near the geomagnetic latitudes of earthquakes.

3.2.3. *Statistics considering samples selected under different criteria*. The findings and analysis presented above may be dependent on the criteria used in this study. Subsets of the data, selected under different criteria, could show different results. For example, a possible influence on the observation of emissions generated by earthquakes may be whether the earthquake occurred below land or water. *Oike and Ogawa* [1986] suggest that emissions are observed only in the case of earthquakes that occur in an inland area or in a shallow water region. Also, earthquakes that occur deep in the crust may not produce observable emissions. The following additional criteria were used to select a subset of earthquake orbits for similar analysis: (1) Earthquakes must have occurred under land. (2) The depth of the earthquakes must have been less than 100 km.

Under these criteria, 10 earthquake orbits and 18 respective control orbits were selected. Additionally, none of these selected orbits occurred during the local time sector 2100-0500, thereby minimizing the likelihood of nighttime natural emissions as discussed in section 2.5. Statistics similar to those of Figure 7 are shown in Figure 11. Even under these criteria, which may be more favorable to the observation of earthquake emissions, no significant difference between earthquake and control orbits was found. Again, minor differences are probably due to the small sample size, which was unavoidable under these criteria. Also, this subset of orbits did not qualitatively exhibit evidence of likely earthquake-related emissions.

Finally, four orbits were obtained which passed near epicenters of magnitude 6.0 or 6.1 earthquakes (the largest earthquakes in this study). Only one of the four orbits exhibits emissions near the epicenter on any channel. The emissions in this case are not strong; furthermore, the earthquake occurred at a depth of 590 km, in a deep ocean area. The other three orbits associated with magnitude ≥ 6.0 earthquakes do not exhibit any emissions above threshold near the epicenter's latitude.

With only 63 possible earthquake orbits from which to draw in this study, severe fractioning of the data set limited the number of

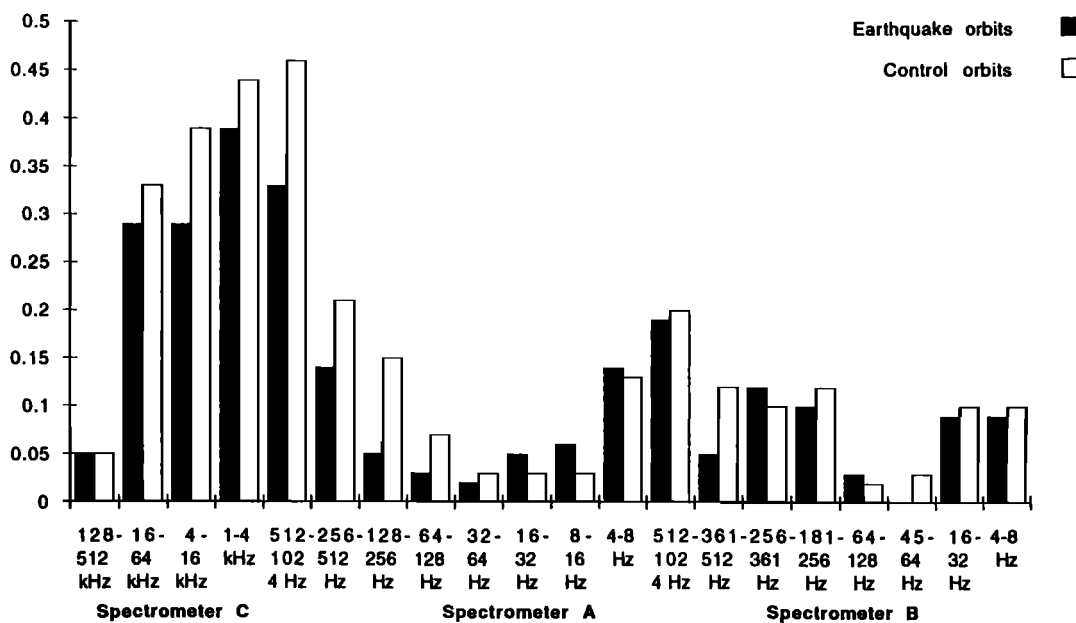


Fig. 7. Fraction of DE 2 orbits that measured an emission in a particular channel.

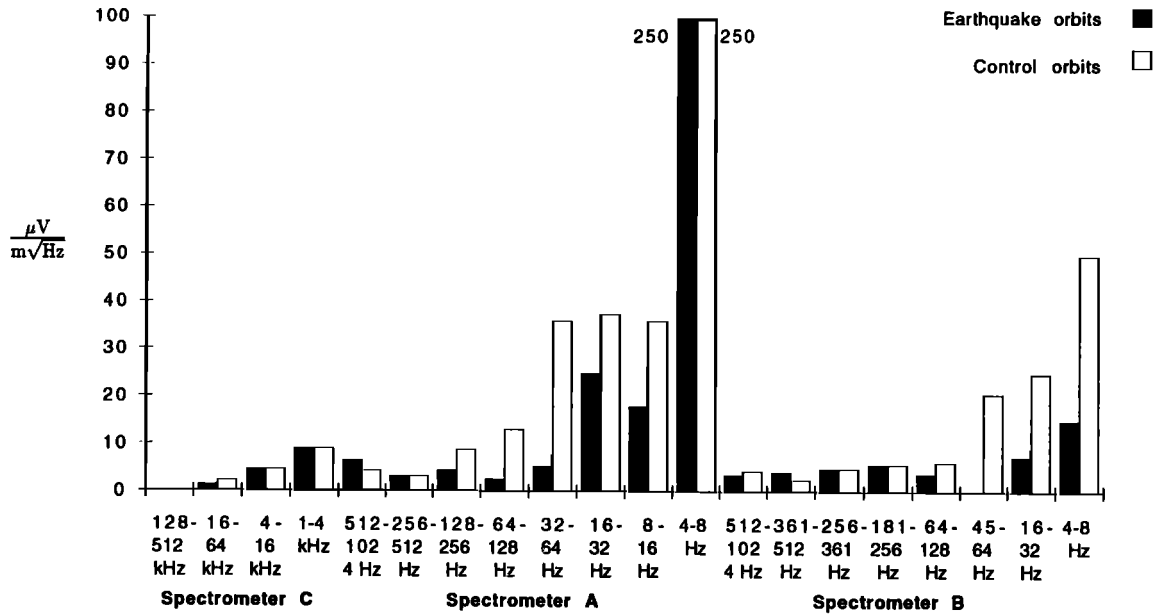


Fig. 8. Normalized peak measurement for the data set considering all orbits, per channel.

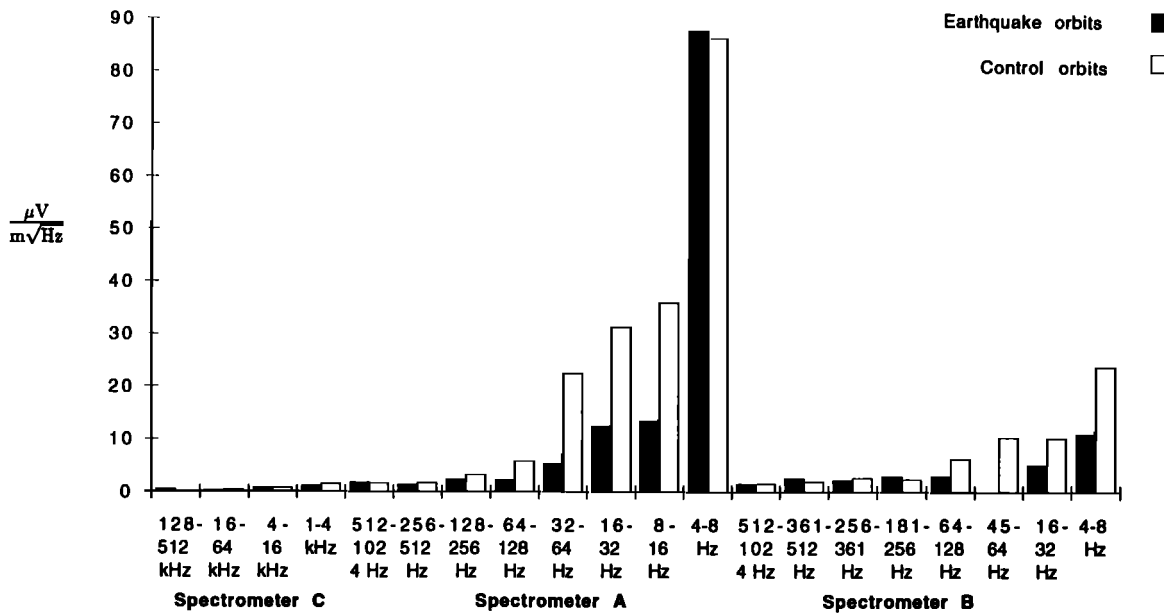


Fig. 9. Normalized emission mean value for all emissions that exceeded 10 μV/m, per channel.

special cases that could be meaningfully examined. For this reason additional investigations must be performed using data from other satellites in order to increase the sample size for these and other interesting subsets of earthquake associated orbits. Such subsets may indicate a correlation between emissions and earthquakes.

4. SUMMARY AND CONCLUSIONS

ELF/VLF wave data from 63 DE 2 orbits coincident with large (magnitude ≥5.0) earthquakes have been examined individually and compared with control orbits not coincident with earthquakes. No unusual emissions, coincident with the passing of the DE 2 satellite near an epicenter within a certain temporal and spatial window, were identified for any orbit. Approximately 63% of the

orbits showed an ELF or VLF emission above 10 μV/m in at least one of the 20 channels when the satellite passed near an epicenter; 37% were quiet in all channels.

In addition to the 63 orbital passes near earthquake activity, 61 control orbits were examined. Control orbits were selected to match, in terms of geographic and geomagnetic parameters of the orbital track, as completely as possible with the orbits near earthquakes, but for days on which there were no reported earthquakes near the orbital track. Using the same analysis as that performed on the earthquake orbits, no significant differences were found between earthquake orbits and control orbits with regard to frequency of emissions, general spectral form, or peak or mean values of the emissions. For example, as mentioned above, 63%

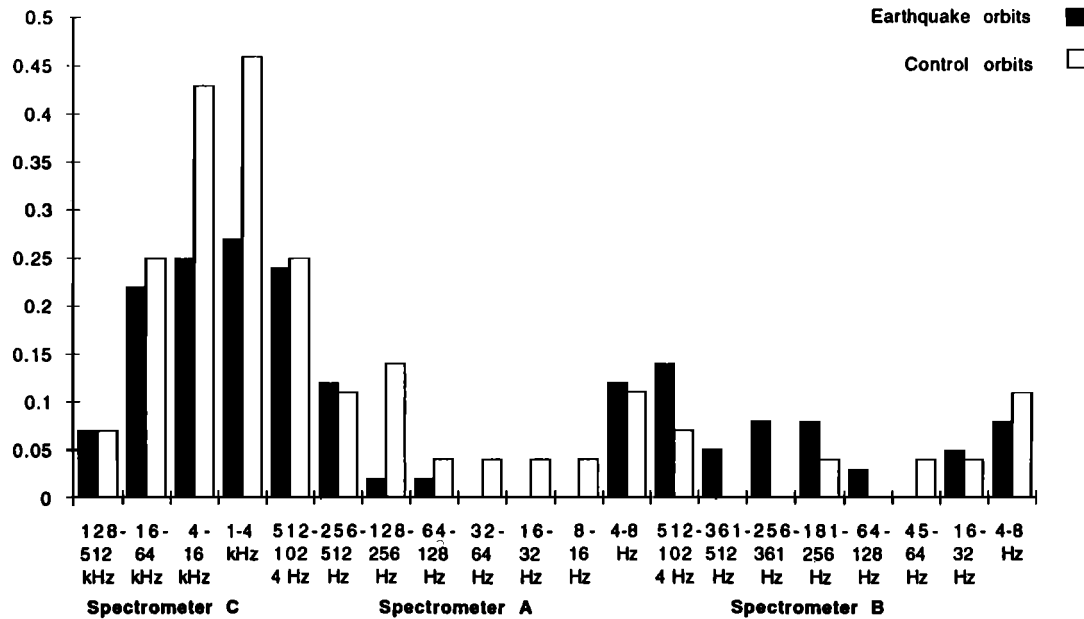


Fig. 10. Fraction of DE 2 orbits that measured an emission in a particular channel for 41 earthquake orbits (and their respective 28 control orbits) at the time when the satellite's magnetic footprint crossed the magnetic latitude of an epicenter.

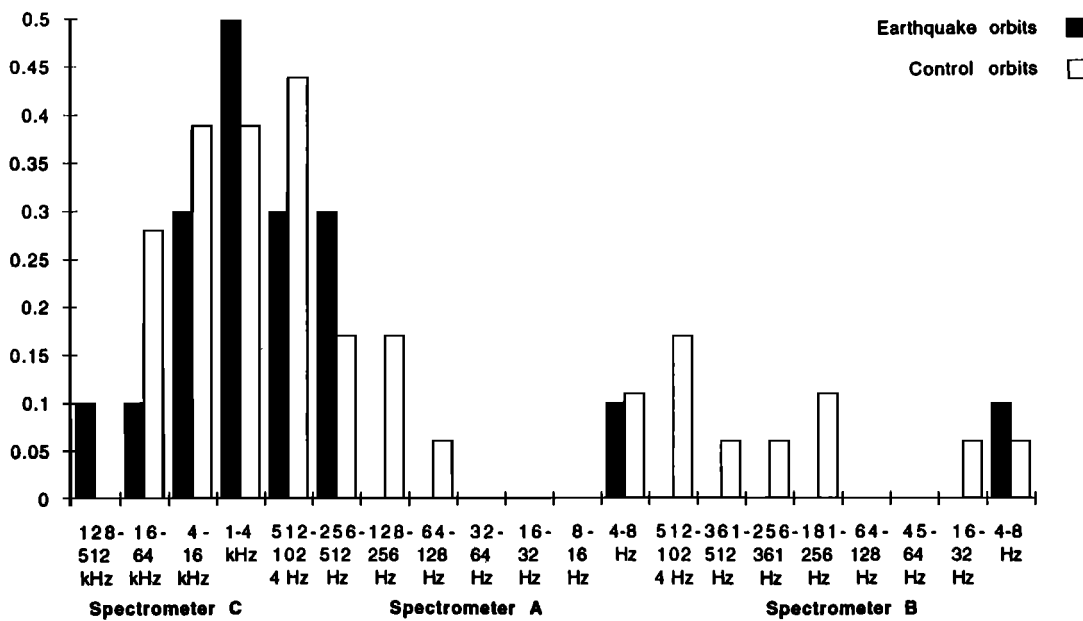


Fig. 11. Fraction of DE 2 orbits that measured an emission in a particular channel for 10 earthquake orbits (and their respective 18 control orbits) in which the earthquake occurred below land and at a depth of less than 100 km.

of the earthquake orbits registered ELF/VLF emissions of some kind near earthquake epicenters. The same analysis performed on control orbits yielded a 62% chance of similar emissions.

Although clear signatures distinct from the background emissions that normally occur were not observed, it is possible that earthquake-induced emissions have signatures that cannot be distinguished from normal background emissions. In that case, however, if so, emissions in general should occur more often during the earthquake orbits, which was not true in this data set.

While this work does not verify the previous claims of electromagnetic precursors to earthquakes, it does not eliminate the possibility of such a phenomenon. These results, however, clearly point out the difficulties involved in confirming such a claim based

on ionospheric observations in the ELF/VLF frequency bands and suggest directions for future work.

The observation of potential earthquake precursors in the ionosphere is a relatively young field. As this paper exemplifies, the existence and the possibility of satellite detection of such precursors remains open to scientific debate. Examination of additional data from other similar low-altitude satellites would contribute most to the search for ELF/VLF emissions associated with earthquakes. As was emphasized above, the analysis of adequate amounts of control data will remain critical to the proper identification of emissions. More detailed observations, such as those from a wideband receiver or from multiple antennas, could possibly be performed with other low-altitude satellites. Very large

earthquakes may exhibit emissions of the kind previously reported with regularity; other satellite data should be searched, and even combined, in order to obtain a larger sample size for such special cases. Nonseismic sources of ELF/VLF waves, such as wave particle interactions or thunderstorm activity, should be considered when looking at individual cases. Finally, VLF emissions from the moon or other planets exhibiting seismic activity might be considered, especially in extraterrestrial cases with low-average ELF/VLF background emissions.

Substantial contributions can also be made in the form of theoretical models for the physical realization of possible mechanisms for seismic emissions [Larkina *et al.*, 1989; Parrot and Mogilevsky, 1989; Draganov *et al.*, 1991]. Discussions of mechanisms for ELF/VLF wave production and propagation due to seismic activity are beyond the scope of this study.

Acknowledgments. We gratefully acknowledge the helpful comments of N. C. Maynard, principal investigator for the VEFI experiment, of the Geophysics Directorate of the Phillips Laboratory, Hanscom Air Force Base. We also thank N.C. Maynard for his assistance in obtaining complete VEFI plots, C. Liebrecht of STX Systems Corporation for producing a large number of VEFI plots for this study, and J. Yarborough of Stanford University for producing spectral plots from the DE 1 spacecraft. Finally, we thank the referees for their useful comments on the manuscript. This research was sponsored by the National Aeronautics and Space Administration under contract NAGS-476 and by the Office of Naval Research (ACFS) through ONR Grant No. N00014-92-J-1576.

The editor thanks N. C. Maynard and M. Parrot for their assistance in evaluating this paper.

REFERENCES

- Chmyrev, V. M., N. V. Isaev, S. V. Bilichenko, and G. Stanev, Observation by space-borne detectors of electric fields and hydromagnetic waves in the ionosphere over an earthquake center, *Phys. Earth Planet. Inter.*, **57**, 110-114, 1989.
- Draganov, A. B., U. S. Inan, and Yu. N. Taranenko, ULF magnetic signatures at the earth surface due to ground water flow; a possible precursor to earthquakes, *Geophys. Res. Lett.*, **18**, 6, 1127-1130, 1991.
- Fraser-Smith, A. C., A. Bernardi, P. R. McGill, M. E. Ladd, R. A. Helliwell, and O. G. Villard, Jr., Low-frequency magnetic field measurements near the epicenter of the Ms 7.1 Loma Prieta earthquake, *Geophys. Res. Lett.*, **17**, 1465, 1990.
- Gokhberg, M. B., V. A. Morgunov, and Y. L. Aronov, Radiofrequency radiation during earthquakes, *Dokl. Akad. Nauk. SSSR*, **248**, 32-35, 1981.
- Gokhberg, M. B., V. A. Morgounov, T. Yoshino, and I. Tomizawa, Experimental measurement of electromagnetic emissions possibly related to earthquakes in Japan, *J. Geophys. Res.*, **87**, 7824-7828, 1982a.
- Gokhberg, M. B., V. A. Pilipenko, and O. A. Pokhotelov, Satellite observation of electromagnetic radiation over the epicentral region of an imminent earthquake, *Dokl. Akad. Nauk. SSSR*, **268**, 56-58, 1982b.
- Hoffman, R. A., G. D. Hogan, and R. C. Maehl, Dynamics Explorer spacecraft and ground operations systems, *Space Sci. Instrum.*, **5**, 349-367, 1981.
- Holtet, J. A., N. C. Maynard, and J. P. Heppner, Variational electric fields at low latitudes and their relation to spread-F and plasma irregularities, *J. Atmos. Terr. Phys.*, **39**, 247-262, 1977.
- Kelley, M. C. and F. S. Mozer, A satellite survey of vector electric fields in the ionosphere at frequencies of 10 to 500 hertz: 3. Low-frequency equatorial emissions and their relationship to ionospheric turbulence, *J. Geophys. Res.*, **77**, 4183-4189, 1972.
- Larkina, V. I., A. V. Nalivano, N. I. Gershenzon, M. B. Gokhberg, V. A. Liperovskiy, and S. L. Shalimov, Observations of VLF emission, related with seismic activity, on the Intercosmos-19 satellite, *Geomagn. and Aeron., Engl. Transl.*, **23**, 684-687, 1983.
- Larkina, V. I., V. V. Migulin, O. A. Molchanov, I. P. Kharkov, A. S. Inchin, and V. B. Schvetcova, Some statistical results on very low frequency radiowave emissions in the upper ionosphere over earthquake zones, *Phys. Earth Planet. Inter.*, **57**, 100-109, 1989.
- Maki, K., and T. Ogawa, ELF emissions associated with earthquakes, *Res. Lett. Atmos. Electr.*, **3**, 41-44, 1983.
- Maynard, N. C., E. A. Bielecki, and H. F. Burdick, Instrumentation for vector electric field measurements from DE-B, *Space Sci. Instrum.*, **5**, 523-534, 1981.
- Oike, K. and T. Ogawa, Electromagnetic radiation from shallow earthquakes observed in the LF range, *J. Geomagn. Geoelectr.*, **38**, 1031-1040, 1986.
- Parrot, M., and F. Lefeuvre, Correlation between GEOS VLF emissions and earthquakes, *Ann. Geophys.*, **3**, 6, 733-748, 1985.
- Parrot, M., and M. M. Mogilevsky, VLF emissions associated with earthquakes and observed in the ionosphere and the magnetosphere, *Phys. Earth Planet. Inter.*, **57**, 86-99, 1989.
- Serebryakova, O. N., S. V. Bilichenko, V. M. Chmyrev, M. Parrot, J. L. Rauch, F. Lefeuvre, and O. A. Pokhotelov, Electromagnetic ELF radiation from earthquake regions as observed by low-altitude satellites, *Geophys. Res. Lett.*, **19**, 91-94, 1992.
- Tate, J., and W. Daily, Evidence of electro-seismic phenomena, *Phys. Earth Planet. Inter.*, **57**, 1-10, 1989.

T. R. Henderson, COMSAT Laboratories, Clarksburg, MD 20871.
A. C. Fraser-Smith, R. A. Helliwell, U. S. Inan and V. S. Sonwalkar, STAR Laboratory, Department of Electrical Engineering, Stanford University, Stanford, CA 94305.

(Received November 25, 1991;
revised April 13, 1992;
accepted May 20, 1992.)